

Electron-, Proton-, and Photon-Induced Spectroscopic Changes in Chromophore-Quencher Tricarbonyl(2,2'-Bipyridine)rhenium(I) Complexes with 4,4'-Azobis(pyridine)

Gaston Pourrieux,[†] Florencia Fagalde,[†] Isabel Romero,[‡] Xavier Fontrodona,[‡] Teodor Parella,[§] and Néstor E. Katz^{*,†}

[†]*INQUINOA-CONICET, Instituto de Química Física, Facultad de Bioquímica, Química y Farmacia, Universidad Nacional de Tucumán, Ayacucho 491, (T4000INI) San Miguel de Tucumán, Argentina,*

[‡]*Departament de Química and Serveis Tècnics de Recerca (STR), Universitat de Girona, Campus de Montilivi, E-17071 Girona, Spain, and* [§]*Servei de RMN, Universitat Autònoma de Barcelona, Bellaterra E-08193, Barcelona, Spain*

Received September 24, 2009

We report in this work the synthesis and characterization of new mono- and dinuclear complexes of formulas: $[\text{Re}(\text{bpy})(\text{CO})_3(4,4'\text{-azpy})](\text{CF}_3\text{SO}_3)$, **1** (bpy=2,2'-bipyridine, 4,4'-azpy=4,4'-azobis(pyridine)); $(\text{bpy})(\text{CO})_3\text{Re}(4,4'\text{-azpy})\text{Ru}(\text{NH}_3)_5(\text{PF}_6)_3 \cdot \text{CH}_3\text{CN} \cdot 6\text{H}_2\text{O}$, **2** and the heterodinuclear species $[(\text{bpy})(\text{CO})_3\text{Re}(4,4'\text{-azpy})\text{Ru}(\text{NH}_3)_5]^{4+}$, **3** (obtained in situ by electrochemical oxidation of **2**). The molecular structure of **1** has been determined by X-ray diffraction. We also report the effect of controlled potential electrolysis, protonation, and light excitation on the absorption and emission properties of these complexes. In particular, complex **1**, which is almost non-emissive at room temperature, recovers luminescence either by reduction of coordinated 4,4'-azpy or by *trans*- to *cis*-photoisomerization. The detected emission of **1** at 77 K is due to decay from a $\text{Re} \rightarrow \text{bpy}$ metal-to-ligand charge transfer excited state. Time dependent density functional theory calculations support the interpretation of the photophysical changes induced by external stimuli.

Introduction

Polypyridyl transition metal complexes containing organic ligands capable of changing their structures reversibly in response to external stimuli (i.e., applied potential, H^+ , light, etc.) have received special attention because of their behavior as “molecular switches” in nanoscopic devices.¹ We have recently described several tricarbonylpolypyridylrhenium(I) complexes with nitrogen heterocyclic ligands L of the type $[\text{Re}(\text{bpy})(\text{CO})_3(\text{L})]^+$ (bpy = 2,2'-bipyridine; L = 4-pyridineal-dazine) that can be used as pH sensors through absorption or emission measurements.² Thus, the combination of an emissive chromophore such as $\text{Re}(\text{bpy})(\text{CO})_3$ with a suitable quencher L may result in electron-, proton-, or photon-induced spectroscopic changes that can be used in designing

molecular switching devices. In particular, the ligand L = 4,4'-azpy or 4,4'-azobis(pyridine) can be isomerized between two conformational states (*trans* \rightarrow *cis*) by light excitation.³ There is also the possibility of changes in physicochemical properties induced by protonation at the pyridinic or azo nitrogens. Besides, the azo functional group ($-\text{N}=\text{N}-$) is responsible for part of the redox activity observed upon electron uptake.⁴ This ligand can also behave as a conducting bridge in “molecular wires”, as recently reported for several ruthenium polypyridyl complexes with 4,4'-azpy.⁵ With the objective of disclosing externally induced spectroscopic changes in rhenium(I) complexes that include 4,4'-azpy in their molecular structure, we report in this work the synthesis and characterization of new mono- and dinuclear complexes with the following formulas: $[\text{Re}(\text{bpy})(\text{CO})_3(4,4'\text{-azpy})](\text{CF}_3\text{SO}_3)$, **1**; $(\text{bpy})(\text{CO})_3\text{Re}(4,4'\text{-azpy})\text{Ru}(\text{NH}_3)_5(\text{PF}_6)_3 \cdot \text{CH}_3\text{CN} \cdot 6\text{H}_2\text{O}$, **2**, and the heterodinuclear species $[(\text{bpy})(\text{CO})_3\text{Re}(4,4'\text{-azpy})\text{Ru}(\text{NH}_3)_5]^{4+}$, **3**. Scheme 1 shows the proposed structure of the

*To whom correspondence should be addressed. E-mail: nkatz@fbqf.unt.edu.ar. Phone: (+54)(381)(4200960). Fax: (+54)(381)(4248169).

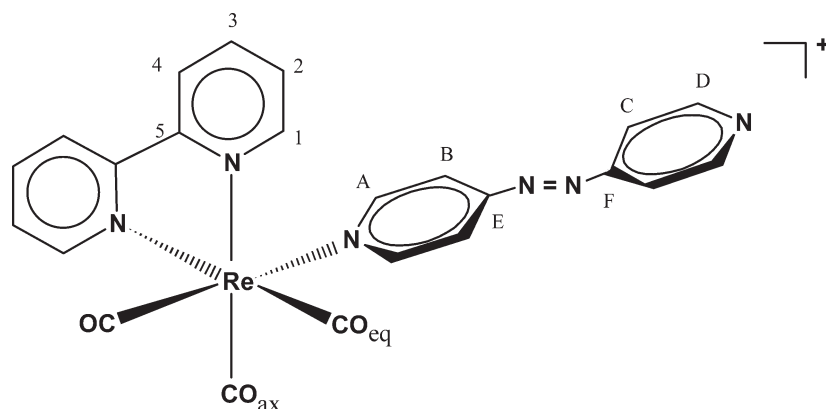
(1) (a) Szacilowski, K. *Chem. Rev.* **2008**, *108*, 3481 and references therein. (b) Kume, S.; Nishihara, H. *Struct. Bonding (Berlin)* **2007**, *123*, 79. (c) Kume, S.; Nishihara, H. *Dalton Trans.* **2008**, 3260. (d) Kumar, A.; Sun, S.-S.; Lees, A. J. *Top. Organomet. Chem.* **2010**, *29*, 1.

(2) (a) Cattaneo, M.; Fagalde, F.; Katz, N. E. *Inorg. Chem.* **2006**, *45*, 6884. (b) Cattaneo, M.; Fagalde, F.; Katz, N. E.; Borsarelli, C. D.; Parella, T. *Eur. J. Inorg. Chem.* **2007**, *34*, 5323. (c) Cattaneo, M.; Fagalde, F.; Borsarelli, C. D.; Katz, N. E. *Inorg. Chem.* **2009**, *48*, 3012.

(3) (a) Yam, V. W.-W.; Lau, V. C.-Y.; Cheung, K.-K. *J. Chem. Soc., Chem. Commun.* **1995**, 259. (b) Yam, V. W.-W.; Lau, V. C.-Y.; Wu, L.-X. *J. Chem. Soc., Dalton Trans.* **1998**, 1461.

(4) Sadler, J. L.; Bard, A. J. *J. Am. Chem. Soc.* **1968**, *90*, 1979.

(5) Pourrieux, G.; Fagalde, F.; Katz, N. E.; Parella, T.; Benet-Buchholz, J.; Llobet, A. *Polyhedron* **2008**, *27*, 2990.

Scheme 1. Structure of $[\text{Re}(\text{bpy})(\text{CO})_3(4,4'\text{-azpy})]^+$ 

cation of complex **1**, which has been confirmed in this study by X-ray crystallography, and the atomic numbering is used for NMR assignment. We also report the effect of controlled potential electrolysis, protonation, and light excitation on the absorption and emission properties of these complexes, and of the previously described³ symmetric complex $[(\text{bpy})(\text{CO})_3\text{Re}(\text{CO})_3(\text{bpy})]^{2+}$.

Experimental Section

Materials and Techniques. All chemicals used in this work were analytical-reagent grade. CH_3CN was freshly distilled over P_4O_{10} for electrochemical measurements. Purification of the complexes was accomplished on silica columns with a flash chromatographic equipment from Büchi, provided with a C/601 pump module and a C/610 flow control unit. Absorption spectra were recorded on a Varian Cary 50 spectrophotometer, using 1 cm quartz cells. Emission measurements were carried out in 1 cm fluorescence cells with a Shimadzu RF-5301 PC spectrofluorometer. Emission at 77 K was measured by using a PTI coldfinger Dewar accessory. Photolysis measurements were performed with this same fluorometer using the largest available slits (20 mm). Infrared spectra were obtained as KBr pellets, with a Perkin-Elmer Spectrum RX-1 FTIR spectrometer. Electrochemistry experiments were carried out using a BAS Epsilon EC equipment for complex **1** and a Zhaner IM6e equipment for complex **2**, with vitreous C as working electrode, Pt wire as auxiliary electrode, and Ag/AgCl (3 M KCl) as reference electrode. All solutions were prepared in CH_3CN , with 0.1 M TBAPF_6 (tetra-*n*-butylammonium hexafluorophosphate) as the supporting electrolyte, and thoroughly degassed with Ar, prior to each experiment. The reported $E_{1/2}$ values were calculated as the averages between the peak values corresponding to the cathodic (E_c) and anodic (E_a) waves: $E_{1/2} = (E_c + E_a)/2$. Controlled potential electrolyses were performed using an OTTLE cell from CH Instruments in CH_3CN (0.1 M TBAPF_6) and a L.Y.P. electrochemical instrument. NMR spectra were obtained in CD_3CN with a Bruker 600 MHz equipment. Electrospray

Ionization (ESI) mass spectra were recorded on a Bruker Esquire 6000 mass spectrometer. Calculations were obtained using Gaussian'98.⁶ The molecules were optimized using Becke's three-parameter hybrid functional B3LYP,⁷ with the local term of Lee, Yang, and Parr.⁸ The basis set LanL2DZ was chosen for all atoms, and the geometry optimizations were performed in the gas phase. Chemical analyses were carried out at INQUIMAE, University of Buenos Aires, Buenos Aires, Argentina, with an estimated error of $\pm 0.5\%$.

Crystal-Structure Determination. Crystals of $\text{C}_{24}\text{H}_{16}\text{N}_6\text{F}_3\text{O}_6\text{ReS}$ were grown from slow diffusion of ethyl ether into a solution of compound **1** in CH_3CN , and used for room temperature (RT, 300(2) K) X-ray structure determination. The measurement was carried out on a BRUKER SMART APEX CCD diffractometer using graphite-monochromated Mo $K\alpha$ radiation ($\lambda = 0.71073 \text{ \AA}$) from an X-ray Tube. The measurements were made in the range 2.70 to 28.62° for θ . Full-sphere data collection was carried out with ω and φ scans. A total of 17357 reflections were collected of which 6396 [$R(\text{int}) = 0.0264$] were unique. Programs used were Smart version 5.631 (Bruker AXS 1997–02) for data collection, Saint+ version 6.36A (Bruker AXS 2001) for data reduction, and SADABS version 2.10 (Bruker AXS 2001) for absorption correction. Structure solution and refinement were done using SHELXTL Version 6.14 (Bruker AXS 2000–2003) program. The structure was solved by direct methods and refined by full-matrix least-squares methods on F^2 . The non-hydrogen atoms were refined anisotropically. The H-atoms were placed in geometrically optimized positions and forced to ride on the atom to which they are attached. Final R indices [$I > 2\sigma(I)$] $R1 = 0.0266$, $wR2 = 0.0662$; R indices (all data): $R1 = 0.0357$, $wR2 = 0.0698$.

Syntheses. The ligand 4,4'-azobis(pyridine) was synthesized following a procedure reported in the literature.⁹ The precursor $[\text{Re}(\text{bpy})(\text{CO})_3(\text{CF}_3\text{SO}_3)]$ was obtained according to known methods.¹⁰

$[\text{Re}(\text{bpy})(\text{CO})_3(4,4'\text{-azpy})](\text{CF}_3\text{SO}_3)$, **1.** A 74 mg portion (0.13 mmol) of $[\text{Re}(\text{bpy})(\text{CO})_3(\text{CF}_3\text{SO}_3)]$ was dissolved in tetrahydrofuran (THF, 15 mL), together with 239 mg (1.3 mmol) of 4,4'-azpy. After heating at reflux and stirring for 3 h, the solution was cooled at RT, and then diethyl ether (100 mL) was added. The orange precipitate formed after chilling overnight was removed by filtration, washed with diethyl ether, and purified by flash chromatography over a silica column with a $\text{CH}_3\text{CN}/\text{CH}_2\text{Cl}_2$ (1:2 v/v) mixture. The first eluted band (orange) was rotoevaporated to 5 mL and then precipitated with diethyl ether.

(6) Frisch, M. J.; Trucks, G. W.; Schlegel, H. B.; Scuseria, G. E.; Robb, M. A.; Cheeseman, J. R.; Zakrzewski, V. G.; Montgomery, J. A.; Stratman, R. E.; Burant, J. C.; Dapprich, S.; Millam, J. M.; Daniels, A. D.; Kudin, K. N.; Strain, M. C.; Farkas, O.; Tomasi, J.; Barone, V.; Cossi, M.; Cammi, R.; Menucci, B.; Pomelli, C.; Adamo, C.; Clifford, S.; Ochterski, J.; Petersson, G. A.; Ayala, P. Y.; Cui, Q.; Morokuma, K.; Malick, D. K.; Rabuck, A. D.; Raghavachari, K.; Foresman, J. B.; Cioslovski, J.; Ortiz, J. V.; Stefanov, B. B.; Liu, G.; Liashenko, A.; Piskorz, P.; Komaromi, I.; Gomperts, R.; Martin, R. L.; Fox, D. J.; Keith, T.; Al-Laham, M. A.; Peng, C. Y.; Nanayakkara, A.; Gonzalez, C.; Challacombe, M.; Gill, P. M. W.; Johnson, B.; Chen, W.; Wong, M. W.; Andres, J. L.; Gonzales, C.; Head-Gordon, M.; Replegle, E. S.; Pople, J. A. *GAUSSIAN 98*, Revision A.6; Gaussian, Inc.: Pittsburgh, PA, 1998.

(7) Becke, A. D. *J. Chem. Phys.* **1993**, *98*, 5648.

(8) Lee, C.; Yang, W.; Parr, R. G. *Phys. Rev. B* **1988**, *37*, 785.

(9) Launay, J.-P.; Tourrel-Pagis, M.; Lipskier, J.-F.; Marvaud, V.; Joachim, C. *Inorg. Chem.* **1991**, *30*, 1033.

(10) Hino, J. K.; Della Ciana, L.; Dressick, W. J.; Sullivan, B. P. *Inorg. Chem.* **1992**, *31*, 1072.

The orange solid obtained was removed by filtration, washed with diethyl ether, dried and stored under vacuum over P_4O_{10} for 1 day. Yield: 53 mg (54%). Chem. Anal. Found: C, 37.8; H, 2.2; N, 11.0; S, 4.6. Calcd. for $C_{24}H_{16}F_3N_6O_6ReS$: C, 37.9; H, 2.1; N, 11.1; S, 4.2. 1H NMR (CD_3CN ; 600.13 MHz) δ (ppm): 9.29 (d, $J = 5.5$ Hz, $2H_H$); 8.87 (d, $J = 6.2$ Hz, $2H_D$); 8.52 (d, $J = 6.7$ Hz, $2H_A$); 8.43 (t, $J = 8.2$ Hz, $2H_4$); 8.31 (dd, $J = 8.2$ and 7.7 Hz, $2H_3$); 7.84 (dd, $J = 5.5$ and 7.7 Hz, $2H_2$); 7.73 (d, $J = 6.2$ Hz, $2H_C$); 7.67 (d, $J = 6.7$ Hz, $2H_B$). ^{13}C NMR: 195.6 (CO_{ax}); 191.6 ($2CO_{ec}$); 157.8 (C_E); 156.5 (C_F); 155.9 ($2C_S$); 154.4 ($2C_A$); 154.0 ($2C_1$); 152.0 ($2C_D$); 141.2 ($2C_3$); 128.9 ($2C_2$); 124.9 ($2C_4$); 118.9 ($2C_B$); 116.0 ($2C_C$). Positive-ion ESI MS: ion clusters at m/z 611 $\{M\}^+$, 427 $\{Re(CO)_3(bpy)\}^+$.

[(bpy)(CO) $_3$ Re(4,4'-azpy)Ru(NH $_3$) $_5$](PF $_6$) $_3$ ·CH $_3$ CN·6H $_2$ O, 2. A solution of $[Re(bpy)(CO)_3(4,4'-azpy)](PF_6)$ (70 mg, 0.092 mmol) in acetone (15 mL) was purged with Ar for 30 min. The other precursor $[Ru(NH_3)_5(H_2O)](PF_6)_2$ (90 mg, 0.184 mmol), prepared as described before,¹¹ was added to this solution, and the resulting mixture was stirred in darkness, for 2 h, under Ar. Deaerated diethyl ether (100 mL) was added, and the cloudy solution was stored in the refrigerator overnight. The formed dark blue precipitate was removed by filtration, washed with diethyl ether (2×10 mL), sorbed onto a Sephadex LH-20 column, and eluted with a CH_3CN/CH_2Cl_2 (3:1 v/v) solution to remove all the unreacted mononuclear complex. The bluish-green portion was then collected using a CH_3CN/CH_2Cl_2 (1:1 v/v) solution as eluent, concentrated to about 5 mL under reduced pressure and precipitated with diethyl ether (50 mL). The bluish-green solid was removed by filtration, washed with diethyl ether, dried and stored under vacuum over P_4O_{10} for 1 day. Yield: 12 mg (10%). Chem. Anal. Found (mean of 3 determinations): C, 21.5; H, 3.7; N, 12.5. Calcd. for $C_{25}H_{46}F_{18}N_{12}O_9P_3ReRu$: C, 21.7; H, 3.4; N, 12.2. 1H NMR (CD_3CN ; 600.13 MHz): 9.29 (d, $J = 5.5$ Hz, $2H_H$); 8.76 (d, $J = 7.1$ Hz, $2H_D$); 8.46 (d, $J = 6.7$ Hz, $2H_A$); 8.43 (t, $J = 8.2$ Hz, $2H_4$); 8.31 (ddd, $J = 1.4, 8.2,$ and 7.7 Hz, $2H_3$); 7.85 (dd, $J = 5.5$ and 7.7 Hz, $2H_2$); 7.71 (d, $J = 6.7$ Hz, $2H_C$); 7.58 (d, $J = 7.1$ Hz, $2H_B$). Positive-ion ESI MS: ion clusters at m/z 901 $\{M \cdot PF_6\}^-$, 611 $\{M - Ru(NH_3)_5\}^+$, 427 $\{Re(CO)_3(bpy)\}^+$.

[(bpy)(CO) $_3$ Re(4,4'-azpy)Ru(NH $_3$) $_5$] $^{4+}$, 3. This heterodinuclear species was obtained in situ by controlled potential electrolysis of an about 10^{-3} M solution of **2** in CH_3CN , as described below.

[(bpy)(CO) $_3$ Re(4,4'-azpy)Re(CO) $_3$ (bpy)](CF $_3$ SO $_3$) $_2$ ·2H $_2$ O, 4. This symmetric dinuclear complex, already described in the literature as a perchlorate salt,³ was obtained as a byproduct during the flash chromatography purification process of **1**. The second band (yellow), eluted only with CH_3OH , was evaporated to 5 mL and then precipitated with diethyl ether. The obtained yellow solid was removed by filtration, washed with diethyl ether, dried and stored under vacuum over P_4O_{10} for 1 day. Yield: 12 mg (7%). Chem. Anal. Found: C, 33.2; H, 1.8; N, 8.5; S, 4.7. Calcd. for $C_{38}H_{28}F_6N_8O_{14}Re_2S_2$: C, 33.3; H, 2.0; N, 8.2; S, 4.7. 1H NMR (CD_3CN ; 600.13 MHz): 9.25 (d, $J = 5.5$ Hz, $4H_H$); 8.50 (d, $J = 7.4$ Hz, $4H_A$); 8.40 (d, $J = 8.5$ Hz, $4H_4$); 8.29 (ddd, $J = 7.7, 8.5,$ and 1.9 Hz, $4H_3$); 7.82 (ddd, $J = 1.4, 5.5,$ and 7.7 Hz, $4H_2$); 7.60 (d, $J = 7.4$ Hz, $4H_B$). ^{13}C NMR: 196.5 ($4CO_{ax}$); 194.4 ($2CO_{ec}$); 158.3 ($2C_E$); 156.9 ($4C_S$); 155.5 ($4C_A$); 154.9 ($4C_1$); 142.2 ($4C_3$); 129.8 ($4C_2$); 125.7 ($4C_4$); 120.0 ($4C_B$). Positive-ion ESI MS: ion clusters at m/z 1186 $\{M \cdot CF_3SO_3\}^+$, 611 $\{M - Re(CO)_3(bpy)\}^+$, 427 $\{Re(CO)_3(bpy)\}^+$.

Results and Discussion

Syntheses, NMR, and IR Spectra. The synthetic procedures follow protocols previously described for tricarbonylpolypyridylrhenium(I) complexes with nitrogen heterocycles.² As a novelty, we have introduced in this work

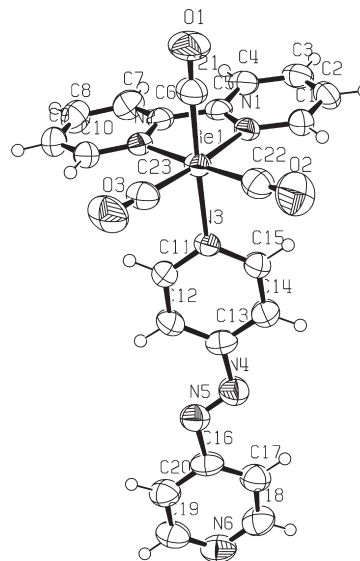


Figure 1. ORTEP diagram (ellipsoids at 70% probability) of $[Re(bpy)(CO)_3(4,4'-azpy)]^+$, with labeling scheme for all atoms (excepting H).

flash chromatography as a purification technique. The IR spectra for the solid samples of complexes **1** and **2** display the characteristic vibrational modes of the polypyridyl ligands (bpy and 4,4'-azpy) and two intense bands in the region 2034 – 1936 cm^{-1} , corresponding to the carbonyl groups stretching frequencies, $\nu_{C=O}$. The values of these latter frequencies are close to those reported for related complexes.² Complex **2** also displays the ammonia symmetric deformation mode $\delta_{sym}(NH_3)$ at 1267 cm^{-1} , a value characteristic of pentaammineruthenium(II) moieties.⁵ The NMR spectral data for complex **1** are consistent with the *trans*-structure disclosed by the crystal structure. The numbering of atoms of the NMR spectrum of **1** follows the assignment of Scheme 1. There is a symmetry plane containing one CO group, the Re atom, and the 4,4'-azpy moiety. ^{13}C NMR spectrum of **1** indicates the presence of two types of CO groups (in a 2:1 proportion at 195.6 and 191.6 ppm respectively).

Crystal Structure. Figure 1 shows an ORTEP diagram for the cation of **1**. A *trans*-structure for the 4,4'-azpy ligand is disclosed in this complex, as already determined in analogous polypyridylruthenium(II) species.⁵ Besides, an interesting moderately weak π – π stacking between adjacent 4,4'-azpy ligands is operative, as shown in Figure 2. The plane-to-plane distance has been estimated as 6.93 Å. Similar π – π interactions have been detected before in transition metal complexes of 4,4'-azpy.¹² In contrast, the ion $[Ru(trpy)(bpy)(4,4'-azpy)]^{2+}$ ($trpy = 2,2':6',2''$ -terpyridine) shows much more extensive π – π stacking because of the interaction of neighboring polypyridyl ligands.⁵

Some selected bond lengths and angles are shown in Table 1. The presence of two types of CO groups is clearly confirmed. The N–N distance of the azo group (1.204 Å) is typical for a *trans*-configuration, as confronted to the

(11) Sutton, J. E.; Taube, H. *Inorg. Chem.* **1981**, *20*, 3125.

(12) (a) Li, B.; Liu, H.; Xu, Y.; Chen, J.; Wang, H.; Xu, Z. *J. Mol. Struct.* **2001**, *597*, 21. (b) Li, B.; Lang, J.; Ding, J.; Zhang, Y. *Inorg. Chem. Commun.* **2003**, *6*, 141. (c) Noro, S-i.; Kitagawa, S.; Nakamura, T.; Wada, T. *Inorg. Chem.* **2005**, *44*, 3960.

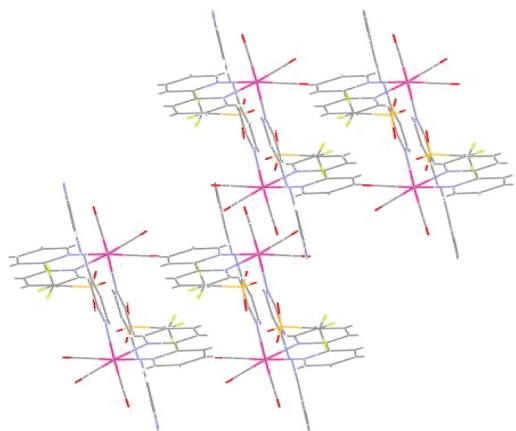


Figure 2. View of the crystal packing of $[\text{Re}(\text{bpy})(\text{CO})_3(4,4'\text{-azpy})]^+$.

Table 1. Selected Bond Distances and Angles for the Cation of **1**

| bond distances (Å) | | bond angles (deg) | |
|--------------------|----------|-------------------|------------|
| Re(1)–C(23) | 1.913(4) | C(23)–Re(1)–C(21) | 90.10(15) |
| Re(1)–C(22) | 1.917(4) | C(23)–Re(1)–C(22) | 88.65(17) |
| Re(1)–C(21) | 1.924(4) | C(21)–Re(1)–C(22) | 88.19(17) |
| Re(1)–N(2) | 2.176(3) | C(23)–Re(1)–N(2) | 97.04(14) |
| Re(1)–N(1) | 2.185(3) | C(21)–Re(1)–N(2) | 93.41(14) |
| Re(1)–N(3) | 2.216(3) | C(22)–Re(1)–N(2) | 174.08(13) |
| N(4)–N(5) | 1.204(4) | C(23)–Re(1)–N(1) | 171.87(13) |
| | | C(21)–Re(1)–N(1) | 90.18(13) |
| | | C(22)–Re(1)–N(1) | 99.48(14) |
| | | N(2)–Re(1)–N(1) | 74.83(10) |

Table 2. Electronic Absorption Data of the Cations of Complexes **1–3**, in CH_3CN

| complex | $(10^{-3} \lambda_{\text{max}}, \text{nm})$ $(10^{-3} \epsilon_{\text{max}}, \text{M}^{-1} \text{cm}^{-1})$ |
|---|--|
| $[\text{Re}(\text{bpy})(\text{CO})_3(4,4'\text{-azpy})]^+$ | 251 sh (20.0); 276 (23.2); 303 sh (18.4); 320 (18.4); 335 sh (9.8) |
| $[(\text{bpy})(\text{CO})_3\text{Re}^{\text{I}}(4,4'\text{-azpy})\text{Ru}^{\text{II}}(\text{NH}_3)_5]^{3+}$ | 251 sh (21.4); 273 (23.0); 303 sh (15.5); 321 (14.9); 351 (7.6); 734 (8.3) |
| $[(\text{bpy})(\text{CO})_3\text{Re}^{\text{I}}(4,4'\text{-azpy})\text{Ru}^{\text{III}}(\text{NH}_3)_5]^{4+}$ | 263 (23.4); 303 (17.6); 319 (17.6); 343 (9.2); 584 (0.8) |

distance observed in complexes with 4,4'-azpy in a *cis*-configuration ($\approx 1.4 \text{ \AA}$).¹³

UV–visible Spectroscopy. Table 2 shows the absorption spectral data of the cations of complexes **1–3** in CH_3CN . The UV–visible spectra of the cations of **1** and **2** are shown overlaid in Figure 3. In both cases, the bands between 200 and 320 nm are assigned to intraligand (IL) $\pi \rightarrow \pi^*$ transitions of the polypyridyl ligands (bpy and 4,4'-azpy).⁵ Sharp peaks around 320 nm are characteristic of rhenium(I)-diimine complexes.² The shoulders at $\lambda_{\text{max}} = 335 \text{ nm}$ in **1** and at 351 nm in **2** can be assigned to overlapping metal-to-ligand charge transfer (MLCT) transitions $d_{\pi}(\text{Re}) \rightarrow \pi^*(\text{bpy})$ and $d_{\pi}(\text{Re}) \rightarrow \pi^*(4,4'\text{-azpy})$ in both complexes.² The shift to lower energies in **2** can be ascribed to the electron-withdrawing effect induced by metalation of the remote pyridinic N of bridging 4,4'-azpy. The lowest energy band at $\lambda_{\text{max}} = 734 \text{ nm}$ in **2** can be assigned to a $d_{\pi}(\text{Ru}) \rightarrow \pi^*(4,4'\text{-azpy})$ MLCT transition from the Ru atom bonded to NH_3 . These results are

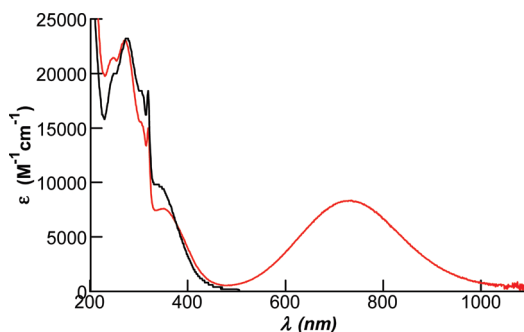


Figure 3. UV–visible spectra of $[\text{Re}(\text{bpy})(\text{CO})_3(4,4'\text{-azpy})]^+$ (black line) and $[(\text{bpy})(\text{CO})_3\text{Re}(4,4'\text{-azpy})\text{Ru}(\text{NH}_3)_5]^{3+}$ (red line) in CH_3CN at RT.

Table 3. Electrochemical Data for the Cations of **1** and **2**, in CH_3CN , at $v = 100 \text{ mV/s}$

| complex | process | $E_{1/2}/\text{V}^a$ | $\Delta E_{1/2}/\text{mV}$ |
|--|---------------------------|----------------------|----------------------------|
| $[\text{Re}(\text{bpy})(\text{CO})_3(4,4'\text{-azpy})]^+$ | $\text{Re}^{2+/+}$ | 1.76 ^b | irr. |
| | $4,4'\text{-azpy}^{0/-}$ | –0.53 | 82 |
| | $4,4'\text{-azpy}^{-/2-}$ | –0.90 | 101 |
| | $\text{bpy}^{0/-}$ | –1.27 | 83 |
| $[(\text{CO})_3(\text{bpy})\text{Re}^{\text{I}}(4,4'\text{-azpy})\text{Ru}^{\text{II}}(\text{NH}_3)_5]^{3+}$ | $\text{Re}^{2+/+}$ | 1.76 ^b | irr. |
| | $\text{Ru}^{3+/2+}$ | 0.46 | 120 |
| | $4,4'\text{-azpy}^{0/-}$ | –0.50 | 79 |
| | $4,4'\text{-azpy}^{-/2-}$ | –0.82 | 99 |
| | $\text{bpy}^{0/-}$ | –1.28 | 119 |

^a $E_{1/2}$ values are referred to SCE. ^b $E_{1/2} = E_c$.

consistent with those reported by us in polypyridylruthenium complexes containing 4,4'-azpy; the same MLCT band appears at $\lambda_{\text{max}} = 738 \text{ nm}$ in $[(\text{trpy})(\text{bpy})\text{Ru}(4,4'\text{-azpy})\text{Ru}(\text{NH}_3)_5]^{4+}$.⁵

Electrochemistry. Table 3 shows the redox potentials obtained from the cyclic voltammograms of complexes **1** and **2** in CH_3CN with 0.1 M TBAPF₆, versus SCE. In both complexes, the couple $\text{Re}^{\text{II}}/\text{Re}^{\text{I}}$ displays a value of $E_{1/2} \approx 1.80 \text{ V}$, which is similar to those reported for related complexes.² For complex **2**, there is also a reversible oxidative wave associated to the $\text{Ru}^{\text{III}}/\text{Ru}^{\text{II}}$ couple at $E_{1/2} = 0.46 \text{ V}$. The difference in potentials of both couples is therefore: $\Delta E_{1/2} = E_{1/2}(\text{Re}^{\text{II}}/\text{Re}^{\text{I}}) - E_{1/2}(\text{Ru}^{\text{III}}/\text{Ru}^{\text{II}}) \approx 1.30 \text{ V}$. On the reductive side of the cyclic voltammograms, coordinated bpy displays its characteristic reversible reduction wave at $E_{1/2}$ about -1.30 V , as reported in the literature for similar systems.⁵ In the case of coordinated 4,4'-azpy, its reductions give rise to one reversible peak at $E_{1/2} \approx -0.50 \text{ V}$ and a quasi-reversible peak at $E_{1/2} \approx -0.90 \text{ V}$, as expected for this azo ligand.⁵ As already noted before, the dianion of reduced 4,4'-azpy seems to be more stable than those of other azo compounds.⁴ This property makes the ligand a promising candidate for electroswitching, as confirmed in the spectroelectrochemical experiments (see below).

Controlled Potential Electrolysis of 1. When an external potential $E = -0.8 \text{ V}$ is applied for 5 min in the spectroelectrochemical cell to a $6 \times 10^{-4} \text{ M}$ solution of complex **1** in CH_3CN , the intensity of the IL transitions decreases, and a new band appears at $\lambda_{\text{max}} = 450 \text{ nm}$, as shown in the Supporting Information, Figure 1. This latter band can be assigned to a $\pi-\pi^*$ transition of a radical anion of the 4,4'-azpy ligand, since the maximum has similar values to

(13) Theilmann, O.; Saak, W.; Haase, D.; Beckhaus, R. *Organometallics* 2009, 28, 2799.

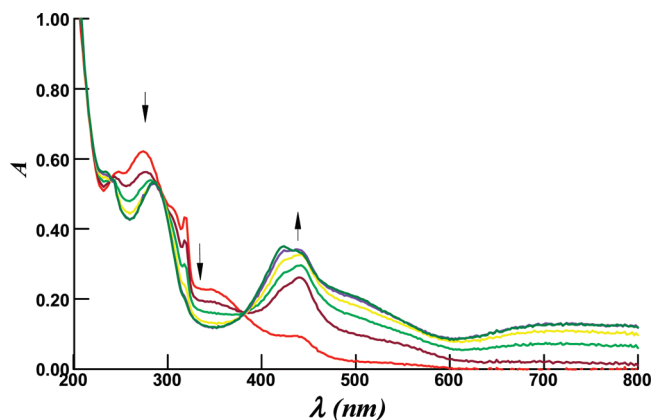


Figure 4. UV/vis absorption changes of **1**, after applying an external potential of $E = -1.0$ V for 8 min. The arrows indicate increasing times from $t = 0$ to $t = 8$ min.

those reported in literature for the IL bands of radical anions of nitrogen ligands.^{14,15} When an external potential $E = -1.0$ V is applied for 8 min in the spectroelectrochemical cell to a 2×10^{-4} M solution of complex **1** in CH_3CN , the intensity of the MLCT band $d_{\pi}(\text{Re}) \rightarrow \pi^*(\text{bpy}, 4,4'\text{-azpy})$ decreases, and the intensity of the band at $\lambda_{\text{max}} = 450$ nm increases noticeably with respect to that of the monoanion, as shown in Figure 4. Besides, new bands appear at wavelengths $\lambda_{\text{max}} > 700$ nm, which may be due to $4,4'\text{-azpy}^{2-} \rightarrow \text{bpy}$ ligand-to-ligand charge transfer (LLCT) transitions, as proposed before.¹⁴ These changes are expected for a doubly reduced radical anion of $4,4'\text{-azpy}$. An isosbestic point is disclosed at 380 nm. After 10 min of electrolysis, a slight decomposition begins, as disclosed by the shifting of this isosbestic point to lower wavelengths.

What is more interesting, when an external potential $E = -1.0$ V is applied, an emission maximum is detected at $\lambda_{\text{em}} = 538$ nm (at $\lambda_{\text{exc}} = 350$ nm), typical of $\text{Re}(\text{I})$ -diimine chromophores, as shown in Figure 5. The absorption and emission changes are reversible: the spectra are restored when the external potential is set back to $E = 0$ V (see Figure 5), which allows us to consider these complexes as *off-on* switches that could be used in the design of nanoscopic devices for molecular electronics.¹ Redox-responsive molecular switches with ruthenium polypyridyls coordinated to azobis(2,2'-bipyridine) have also been described; in these systems, considerable absorption and emission changes have been detected on electron transfer.¹⁶

These phenomena are reproduced in the dinuclear species **4**. The UV/vis absorption changes that occur in a solution of **4** in CH_3CN after applying an external potential of $E = -0.70$ V for 10 min are similar and more reversible than those previously described for complex **1**: the maximum at $\lambda_{\text{max}} = 450$ nm can be assigned to a doubly reduced radical anion of $4,4'\text{-azpy}$. In effect, for this species, the reduction potentials are positively shifted

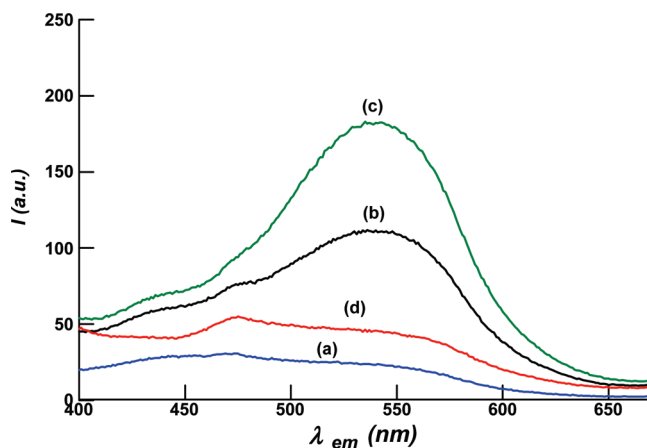


Figure 5. Emission intensity changes of **1**, after applying an external potential of $E = -1.0$ V, at (a) $t = 0$, (b) $t = 5$ min, and (c) $t = 10$ min. Curve (d) is obtained after reverting to $E = 0$ V for 4 min.

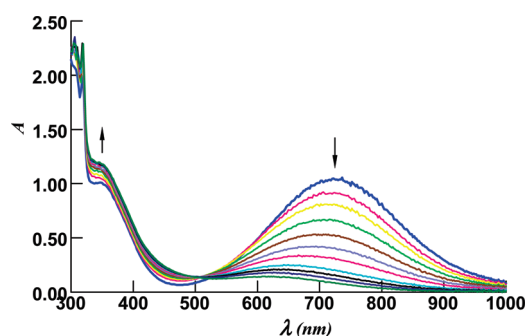


Figure 6. Controlled potential electrolysis of a 1.2×10^{-3} M solution of **2** in CH_3CN at $E = 0.80$ V (optical length = 0.1 cm). The arrows indicate increasing times from $t = 0$ to $t = 10$ min.

by almost 0.2 V with respect to the mononuclear complex. Emission is also enhanced in the doubly reduced species of **4**.

Controlled Potential Electrolysis of 2. As shown in Figure 6, when an external potential $E = 0.80$ V is applied in the spectroelectrochemical cell to a 1.2×10^{-3} M solution of complex **2** in CH_3CN for 10 min, only the ammine-bonded Ru undergoes oxidation to originate the heterodinuclear species **3**, of formula $[(\text{bpy})(\text{CO})_3\text{Re}^{\text{I}}(4,4'\text{-azpy})\text{Ru}^{\text{III}}(\text{NH}_3)_5]^{4+}$. After oxidation of Ru, the band at $\lambda_{\text{max}} = 734$ nm disappears, and a new, weak band at $\lambda_{\text{max}} = 584$ nm appears, which can be assigned to the $[\text{Re}^{\text{I}}, \text{Ru}^{\text{III}}] \rightarrow [\text{Re}^{\text{II}}, \text{Ru}^{\text{II}}]$ intervalence or metal-to-metal charge transfer (MMCT) transition. The process proved to be reversible when a potential of 0 V was applied for 10 min after oxidation.

Gaussian deconvolution of the UV/vis spectrum of **3** in the region 400–1000 nm allowed us to obtain the parameters: $\Delta\nu_{1/2}$ (bandwidth at half-height), ϵ_{max} (molar absorptivity at the absorption maximum), and ν_{max} (energy of the intervalence absorption maximum) of the intervalence band as 7.05×10^3 cm^{-1} , 800 M^{-1} cm^{-1} , and 1.71×10^4 cm^{-1} , respectively. By using these values and applying the Marcus–Hush formalism,¹⁷ which can be successfully applied to both symmetric and unsymmetrical species,¹⁸ the electronic coupling

(14) (a) Kaim, W. *Coord. Chem. Rev.* **1987**, *76*, 187. (b) Kaim, W. *Coord. Chem. Rev.* **2001**, *219–221*, 463.

(15) Katz, N. E.; Mecklenburg, S. L.; Meyer, T. J. *Inorg. Chem.* **1995**, *34*, 1282.

(16) (a) Otsuki, J.; Sato, K.; Tsujino, M.; Okuda, N.; Araki, K.; Seno, M. *Chem. Lett.* **1996**, 847. (b) Otsuki, J.; Omokawa, N.; Yoshida, K.; Yoshikawa, I.; Akasaka, T.; Suenobu, T.; Takido, T.; Araki, K.; Fukuzumi, S. *Inorg. Chem.* **2003**, *42*, 3057.

(17) Creutz, C. *Prog. Inorg. Chem.* **1983**, *30*, 1.

(18) Katz, N. E.; Creutz, C.; Sutin, N. *Inorg. Chem.* **1988**, *27*, 1687.

H_{AB} between both metallic centers in **3** can be calculated using eq 1:

$$H_{AB}(\text{cm}^{-1}) = 2.06 \times 10^{-2} [(\epsilon_{\text{max}})(\tilde{\nu}_{\text{max}})(\Delta\tilde{\nu}_{1/2})]^{1/2} (1/r) \quad (1)$$

where r is the distance (in Å) between both metal centers, estimated as 13.3 Å from the X-ray analysis of **1** and the typical Ru–N bond length for a pentaammineruthenium(III) group coordinated to pyridyl ligands.¹⁹ The final result of the calculation was $H_{AB} \approx 480 \text{ cm}^{-1}$, indicating a moderate interaction, about 20% less than that determined in the heterodinuclear complex [(trpy)(bpy)Ru^{II}-(4,4'-azpy)Ru^{III}(NH₃)₅]⁵⁺.⁵ This decrease is expected when comparing the longer metal–metal distance in a [Ru^I,Ru^{III}] species as compared to that in a [Ru^{II},Ru^{III}] species (see eq 1).

On the other hand, the reorganization energy λ can be calculated as follows:

$$\lambda = E_{\text{op}} - \Delta G^\circ - \Delta E_{\text{exc}} \quad (2)$$

where ΔG° is the free energy difference between both redox centers, assumed as approximately $\Delta E_{1/2} = 1.30 \text{ V}$, and ΔE_{exc} is the energy difference between the excited and ground states, estimated as 0.25 eV for several ruthenium complexes in the event that the MMCT transition results in the population of an excited state.¹⁸ Equation 2 gives $\lambda = 0.6 \text{ eV}$, a value consistent with similar unsymmetrical complexes containing the pentaammineruthenium(III) moiety.⁵

Protonation Studies. A spectrophotometric titration has been carried out by adding aliquots of concentrated HCl to a $2 \times 10^{-5} \text{ M}$ aqueous buffered solution of **1**. The pH was measured in all cases. In the UV/vis region, an increase in absorbance occurs in the IL transitions zone (200–280 nm) with a concomitant decrease in absorbance around the maximum of the MLCT band (350 nm) and a shift of λ_{max} to longer wavelengths (Supporting Information, Figure 2) because of a decrease in energy of the π^* lowest unoccupied molecular orbital (LUMO) of 4,4'-azpy induced by protonation at the free N of coordinated 4,4'-azpy. An isosbestic point is observed around 390 nm. Adding NaOH allows the recovery of the original spectrum, thus confirming the reversibility of this process. As shown in Figure 7, the fitting of absorbance at 358 nm versus pH gives a value of $\text{p}K_{\text{a}} = 3.4 \pm 0.1$, which is readily assigned to the protonation constant of the pyridyl free N of 4,4'-azpy, since it compares very well to that determined in similar complexes, for example, $\text{p}K_{\text{a}} = 3.3 \pm 0.1$ for the same N in [Ru(trpy)(bpy)(4,4'-azpy)]²⁺ (Supporting Information, Figure 3).²⁰

Photolysis. Irradiation of a 10^{-5} M solution of **1** in CH₂Cl₂ for 260 min at wavelengths greater than 350 nm (i.e., 460 nm) increases the emission intensity of the complex by about 50 times, as shown in Figure 8, consistent with results reported in the literature for the photolysis of [Re(bpy)(CO)₃(bpe)]⁺, with bpe = *trans*-1,2-bis(4-pyridyl)ethylene, an isomerizable ligand with a

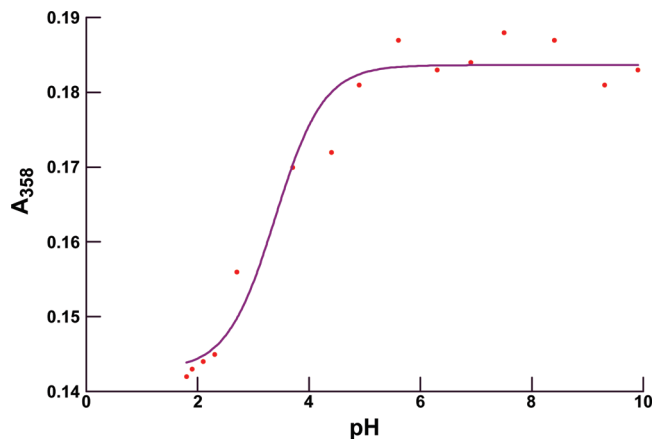


Figure 7. Fitting of absorbance at $\lambda = 358 \text{ nm}$ versus pH of a $2 \times 10^{-5} \text{ M}$ aqueous buffered solution of **1** with different aliquots of HCl added.

–C=C– bond in the center of the molecule,^{21a–c} and with similar axial ligands with a –N=N– bond.^{3,21d} The excited-state dynamics of *trans*-4-phenylazopyridine and 4-styrylpyridine tricarbonyl(2,2'-bipyridine)rhenium(I) complexes²² have been studied in detail; the decay mechanisms of excited states include subpicosecond intersystem crossing to triplets, partial rotation around the double bond, and slower intersystem crossing to the *trans*- or *cis*-ground states. There is also a very fast energy transfer process from the MLCT excited state of the Re(bpy)(CO)₃⁺ chromophore to the intraligand ³ $\pi\pi^*$ state of the axial ligand. In the case of axial ligands containing electron-withdrawing substituents, such as *trans*-*N*-methyl-4,4'-bipyridiniummethylene(Medpe⁺),²³ the situation is more complicated because of the population of the MLCT Re → Medpe⁺. In this work, the emission intensity changes can be accounted for by the photon-induced isomerization of coordinated 4,4'-azpy from a *trans*- to a *cis*- configuration around the –N=N– bond, as already described for mono- and dinuclear rhenium(I) diimine complexes with photoisomerizable ligands.³ This explanation is supported by ³TDDFT calculations, as shown below. It has been recently reported that *trans*- to *cis*-rearrangement of 4,4'-azpy ligands can also be induced by the electronic properties of the metallic fragments.¹³ The luminescence quantum yields for the *trans*- and *cis*-isomers have been determined as $\phi = 0.00038$ and $\phi = 0.019$ respectively, by using [Ru(bpy)₃]²⁺ as standard, and corrected by absorbance and refraction index. These values are similar to those already determined for [Re(CO)₃(bpy)(PHAZO)]⁺, with PHAZO = 4-phenylazopyridine (0.00072 and 0.027, respectively).^{3b} On the other hand, the quantum yield for the observed *trans*–*cis* photoisomerization has been estimated as $\phi_{\text{trans-cis}} \approx 0.6$ by comparing the obtained percentages of both isomers in the stationary state: 64% of *cis* and 36% *trans*; these latter

(21) (a) Itokazu, M. K.; Polo, A. S.; de Faria, D. L. A.; Bignozzi, C. A.; Iha, N. Y. M. *Inorg. Chim. Acta* **2001**, *313*, 149. (b) Itokazu, M. K.; Polo, A. S.; Iha, N. Y. M. *J. Photochem. Photobiol. A* **2003**, *160*, 27. (c) Wenger, O. S.; Henling, L. M.; Day, M. W.; Winkler, J. R.; Gray, H. B. *Inorg. Chem.* **2004**, *43*, 2043. (d) Yutaka, T.; Mori, I.; Kurihara, M.; Mizutani, J.; Tamai, N.; Kawai, T.; Irie, M.; Nishihara, H. *Inorg. Chem.* **2002**, *41*, 7143.

(22) (a) Busby, M.; Matousek, P.; Towrie, M.; Vlček, A., Jr. *J. Phys. Chem. A* **2005**, *109*, 3000. (b) Busby, M.; Matousek, P.; Towrie, M.; Vlček, A., Jr. *Inorg. Chim. Acta* **2007**, *360*, 885.

(23) Vlček, A., Jr.; Busby, M. *Coord. Chem. Rev.* **2006**, *250*, 1755.

(19) Gress, M. E.; Creutz, C.; Quicksall, C. O. *Inorg. Chem.* **1981**, *20*, 1522.

(20) Pourrieux, G.; Fagalde, F.; Katz, N. E. unpublished data.

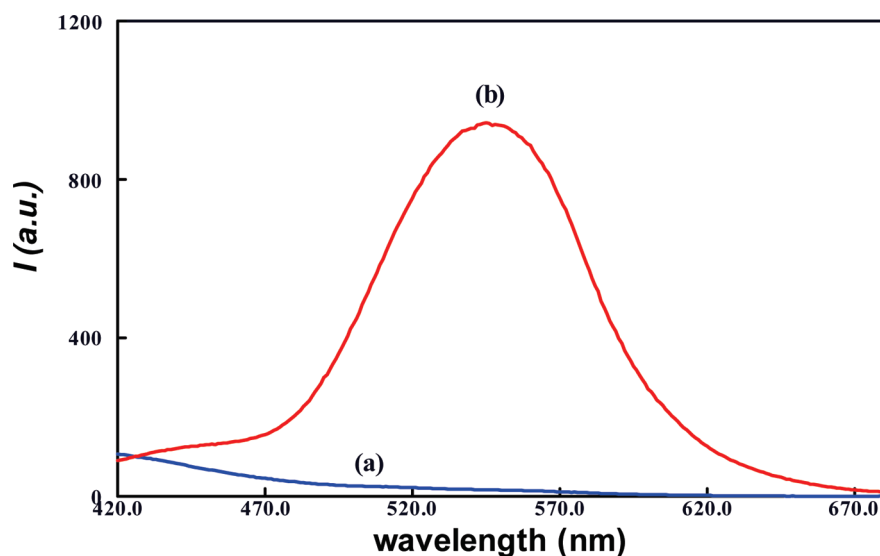


Figure 8. Emission spectra ($\lambda_{\text{ex}} = 350 \text{ nm}$) of a deaerated solution of **1** in CH_2Cl_2 ($C \approx 10^{-5} \text{ M}$): (a) before irradiation and (b) after irradiation, at $\lambda_{\text{irr}} = 460 \text{ nm}$ for 260 min at RT.

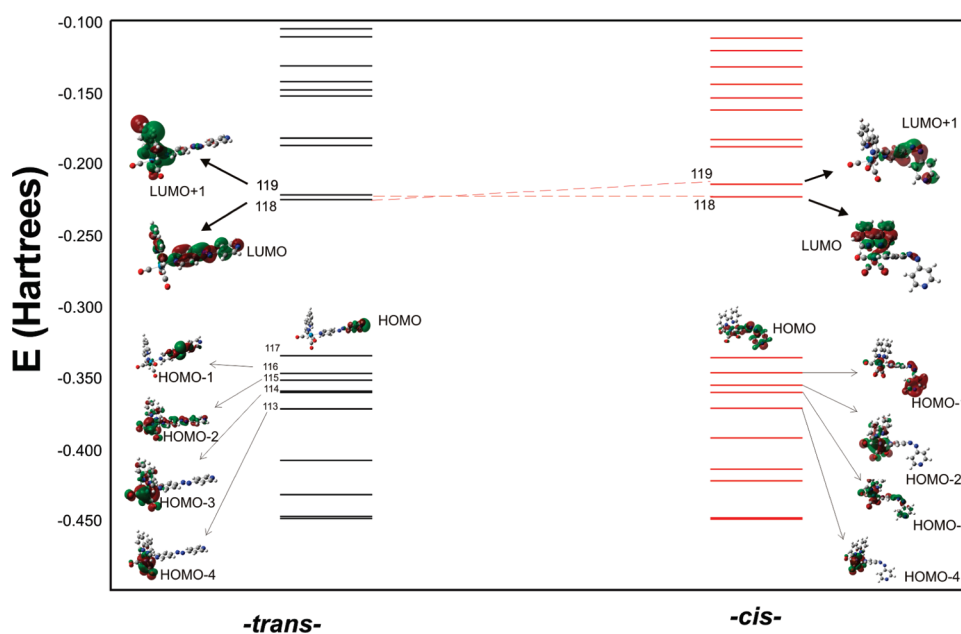


Figure 9. DFT energy levels of $[\text{Re}(\text{bpy})(\text{CO})_3(4,4'\text{-azpy})]^+$ with 4,4'-azpy in the *trans*-configuration (left) and in the *cis*-configuration (right). Forms and approximate description of the frontier orbitals are included.

values resulted from measured UV/vis absorption changes by considering that $\epsilon_{\text{cis}} \approx 0.5\epsilon_{\text{trans}}$, as already determined for similar complexes.^{21c}

Emission Properties and DFT Calculations. The complexes described in this work are very weak emitters at RT. Only the previously studied dinuclear complex **4** shows a moderate quantum yield.³ This quenching effect can be attributed to the presence of the easily reduced 4,4'-azpy ligand. Quantum mechanical calculations can be very helpful to explain physicochemical properties of

Re(I) complexes.²⁴ DFT calculations carried out on the optimized structure of **1** put into evidence, as shown in the left part of Figure 9, that the lowest LUMO is 4,4'-azpy-based, while the LUMO+1 is predominantly bpy-based, in agreement with the electrochemical results. Since emission is due to decay from a $\text{Re} \rightarrow \text{bpy}$ MLCT excited state, rapid energy transfer to ${}^3n\text{-}\pi^*$ 4,4'-azpy-based excited state would explain the almost complete lack of emission in **1**, with 4,4'-azpy in the *trans*-configuration. This possibility is supported by triplet TDDFT calculations: the lowest-energy transition is indeed from ground state to a triplet $n\text{-}\pi^*$ excited state, as shown in Supporting Information, Table 1; these calculations agree with those reported for similar rhenium(I) diimine complexes.^{24a} On the other hand, in the *cis*- isomer, as shown in the right part of Figure 9, there is an inversion of the energy

(24) (a) Vlček, A.; Zális, S. *Coord. Chem. Rev.* **2007**, *251*, 258, and references therein. (b) Kirgen, R.; Simpson, M.; Moore, C.; Day, J.; Bui, L.; Tanner, C.; Rillema, D. P. *Inorg. Chem.* **2007**, *46*, 6464. (c) Machura, B.; Kruszynski, R. *J. Organomet. Chem.* **2007**, *692*, 4161. (d) Zhao, G.-J.; Zhou, X.; Liu, T.; Zheng, Q.-C.; Bai, F.-Q.; Zhang, H.-X. *J. Mol. Struct. THEOCHEM* **2008**, *855*, 52.

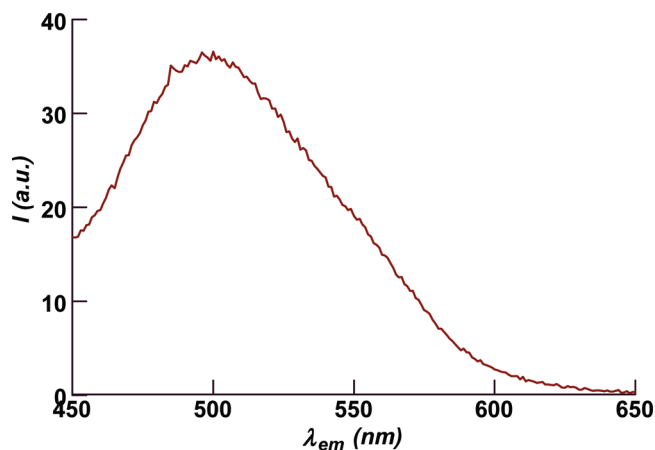


Figure 10. Emission spectra of **1** in an EtOH/MeOH 4:1 glass at 77 K ($\lambda_{\text{ex}} = 350$ nm).

ordering: the LUMO becomes bpy-based and the LUMO+1 is 4,4'-azpy-based; the emission from the lowest-lying Re \rightarrow bpy MLCT excited state is consequently recovered.

The fact that emission originates only from a Re \rightarrow bpy MLCT excited state is also confirmed by luminescence measurements at low temperatures. In effect, at 77 K, as shown in Figure 10, the emission spectrum of **1** ($\lambda_{\text{em}} = 500$ nm at $\lambda_{\text{ex}} = 350$ nm) is characteristic of this excited state, as confronted with the structured emission spectrum expected for a $\pi-\pi^*$ ligand-based excited state.²⁵ Anyways, the intensity is much lower than one would expect at this low temperature, evidencing that crossing to the non-emissive lowest excited state is still operative. The excellent chemical analysis, NMR, MS, and crystal diffraction data obtained for this species exclude possible impurities.

Conclusions

The absorption and emission properties of the chromophore-quencher tricarbonylrhenium(I) complexes with

4,4'-azobis(pyridine) described in this work can be dramatically altered by electron-, proton-, or photon- inputs. In particular, the ion $[\text{Re}(\text{bpy})(\text{CO})_3(4,4'\text{-azpy})]^+$, which is almost non-emissive at RT, can recover its Re \rightarrow bpy MLCT luminescence either by $2e^-$ reduction of coordinated 4,4'-azpy in CH_3CN or by *trans*- to *cis*- photoisomerization in CH_2Cl_2 . On the other hand, the absorption spectrum of the dinuclear complex $[(\text{bpy})(\text{CO})_3\text{Re}^I(4,4'\text{-azpy})\text{Ru}^{II}(\text{NH}_3)_5]^{3+}$ displays large changes induced by $1e^-$ oxidation of coordinated Ru. It should be noted that isomerization induced by light, electrons, or protons have also been reported in ferrocenylazobenzenes.²⁶ We thus conclude that the complexes described in this work can be used in logic circuits at the nanoscopic scale.

Acknowledgment. We thank Universidad Nacional de Tucumán (UNT), Consejo Nacional de Investigaciones Científicas y Técnicas (CONICET), and Agencia Nacional de Promoción Científica y Tecnológica (ANPCyT), all from Argentina, for financial support. F.F and N.E.K. are Members of the Research Career from CONICET, Argentina. G.P. thanks ANPCyT for a graduate fellowship. We also thank Dr. Miriam Pérez (UAB) for the MS measurements.

Supporting Information Available: Crystallographic data in CIF format, UV/vis absorption changes of **1**, after applying an external potential of $E = -0.8$ V for 5 min (Suppl. Figure 1), UV/vis spectrum of $[\text{Re}(\text{bpy})(\text{CO})_3(4,4'\text{-azpy})]^+$ at different pH values (Suppl. Figure 2), fitting of absorbance at 550 nm vs pH of a buffered solution of $[\text{Ru}(\text{trpy})(\text{bpy})(4,4'\text{-azpy})]^{2+}$ (Suppl. Figure 3) and ³TDDFT calculations of 20 lowest-lying electronic transitions of *trans*- $[\text{Re}(\text{bpy})(\text{CO})_3(4,4'\text{-azpy})]^+$ (Suppl. Table 1). This material is available free of charge via the Internet at <http://pubs.acs.org>. Crystallographic data (excluding structure factors) have been deposited with the Cambridge Crystallographic Data Centre as supplementary publication No. CCDC 748907. Copies of the data can be obtained free of charge on application to the CCDC, 12 Union Road, Cambridge CB2 1EZ, U.K. (fax (44) 1223336-033; E-mail: deposit@ccdc.cam.ac.uk).

(25) Cattaneo, M.; Fagalde, F.; Katz, N. E.; Leiva, A. M.; Schmehl, R. *Inorg. Chem.* **2006**, *45*, 127.

(26) Sakamoto, A.; Hirooka, A.; Namiki, K.; Kurihara, M.; Murata, M.; Sugimoto, M.; Nishihara, H. *Inorg. Chem.* **2005**, *44*, 7547.